Gradual phase transition between the smectic-C^* and smectic-C_A^* phases and the thresholdless antiferroelectricity

Jang-Kun Song, Atsuo Fukuda, and J. K. Vij*
Department of Electronic and Electrical Engineering, Trinity College, University of Dublin, Dublin 2, Ireland
(Received 14 May 2008; published 1 October 2008)

We have constructed the phase diagrams for a binary-mixture system of antiferroelectric and ferroelectric liquid-crystalline materials in both thick and thin cells. In the phase diagrams the boundary between the smectic-C^* and smectic-C_A^* phases runs almost parallel to the temperature axis below from ca. 70 °C down to at least −25 °C. The SmC^*-SmC_A^* phase transition for a thin cell shows a large supercooling, and a gradual transition occurs near the boundary. Moreover, the thin cell shows a continuous evolution from the antiferroelectric to the ferroelectric state by increasing the electric field applied across the cell. The continuous evolution seemingly reflects the phenomenon of thresholdless antiferroelectricity. In order to explain these phenomena and in clarifying the mechanism of the so-called frustration between ferroelectricity and antiferroelectricity, we have measured the interlayer interaction energy by varying the constituent concentrations in the binary-mixture system. The measured interlayer interaction close to the boundary indicates that the gradual phase transition and continuous evolution result from the suppression of the solitary-wave propagation by the effect of surfaces.

DOI: 10.1103/PhysRevE.78.041702 PACS number(s): 61.30.Gd, 42.70.Df, 77.84.Nh

I. INTRODUCTION

Antiferroelectric liquid crystals (AFLCs) exhibit tristable switching. This is the electric-field-induced phase transition from anticlinic antiferroelectric SmC_A^* to synclinic ferroelectric SmC^* and is usually characterized by the dc threshold and hysteresis [1]. In addition to such a usual behavior occurring, "thresholdless antiferroelectricity" was suggested [2] as an additional phenomenon while investigating mixtures of compounds. In two apparently AFLC mixtures studied and designated later as the Inui (Tokyo) and the Mitsui mixtures, the thresholdless, hysteresis-free, V-shaped switching was observed to have actually been induced by an applied electric field [3,4] and this observation interested a number of researchers since the phenomenon could potentially be applied to gray-scale displays [5–9]. Two mechanisms were anticipated for the thresholdless switching in AFLCs: (i) A continuous change of the azimuthal angle difference ϕ from the anticlinic to synclinic ordering [10–15] and (ii) the Langevin-like alignment of the azimuthal angle φ_i randomized from layer to layer due to a reduced tilting correlation [2,4,16,17]. Here, $\phi=\varphi_{i+1}-\varphi_i$ and φ_i is the azimuthal angle of the tilting direction for the ith layer. The continuous change of ϕ implies that the free energy, when plotted as a function of ϕ, has only a single minimum for any given value of the applied electric field, and the angle $\phi_{\min}$ corresponding to the minimum energy gradually decreases from anticlinic ($\phi_{\min}\approx\pi$) to synclinic ($\phi_{\min}\approx 0$) by increasing the applied field. In other words, the antiferroelectric state evolves to the ferroelectric state continuously. On the other hand, the Langevin-like alignment of the randomized azimuthal angle presupposes that the free-energy plot has two minima at zero field, one for ferroelectric SmC^* and the other for SmC_A^*, and that both the minima have nearly the same energy value and are separated by an almost negligible energy barrier between them. As a result, any value of ϕ can be thermally excited equally, and thus the frustrated state characterized with randomized azimuthal angle φ_i is realized at zero field. An applied electric field can induce the Langevin-like alignment.

Due to a significant potential of these materials for their use in gray-scale displays, both Mitsubishi Gas Chemical Company, Inc. (MGC) and Mitsui Chemicals, Inc. energetically developed liquid-crystalline compounds and mixtures which showed V-shaped switching [3,4,18–21]. MGC insisted that their developed compounds were *ferrielectric*, and this was based on their observation of conoscopic figures with melatopes appearing parallel to the applied electric field. However, a recent systematic and detailed study by Song *et al.* [22] has clearly revealed that their compounds were unambiguously ferroelectric. As the terminology "thresholdless antiferroelectricity" prevailed at that time in the liquid crystal display community, Mitsui Chemicals simply anticipated that the compounds they developed for V-shaped switching were in their bulk phase antiferroelectric anticlinc SmC_A^* [18]. By taking account of the similarity in the chemical structures of the compounds involved, "Mitsui Chemicals" compounds must be also ferroelctric synclinic SmC^* in their bulk phase, although no detailed study as Song *et al.* performed on MGC compounds has yet been reported on the Mitsui Chemicals compounds. It is now rather clear that ferroelectric liquid crystals with large spontaneous polarization can show thresholdless V-shaped switching [23–27]. In fact, there have been many reports that the Inui (Tokyo) mixture is ferroelectric but not antiferroelectric in the bulk [28–31]. Quite recently, Manjuladevi *et al.* also reported that ferroelectric liquid-crystal materials with large spontaneous polarization and helical compensated pitch show V-shaped switching [32,33]. Hence, we suggest that thresholdless V-shaped switchings observed in MGC and Mitsui compounds may actually correspond to ferroelectric V-shaped switching.

*jvij@tcd.ie

Now, we can retrospectively remark that both companies did adopt the same strategy of enhancing the frustration in preparing their optimized binary mixtures of antiferroelectric and "ferroelectric" liquid-crystal compounds for observing thresholdless antiferroelectricity. In the temperature-concentration (T-x) phase diagram of the binary mixtures, the boundary between SmC_A^* and SmC^* is seen to be rather vertical and runs parallel to the ordinate temperature axis as contrasted with the boundary in the ordinary binary mixtures which usually slants significantly. Close to the boundary for the critical concentration where an almost vertical line crosses the abscissa concentration axis, both SmC_A^* and SmC^* have nearly the same free energies and, hence, frustration between the two is expected. Such a strategy seems to have been adopted rather from the beginning by the Mitsui as well as the Inui mixtures [4,34]. Gorecka *et al.* and Pociecha *et al.* reported the frustration phenomenon in an intermediate range of concentrations for the binary mixtures using C12 and C13 compounds [35,36]. They observed that the polar properties of the phase gradually evolve from antiferroelectric like to ferroelectric like over a wide range of temperatures. This continuous evolution of the polar character has been suggested to arise from the frustration between the antiferroelectric and ferroelectric phases and from the formation of clusters of both phases, which might result from the weak dependence of the interlayer interactions on ϕ. The frustration was anticipated to have been influenced not only by the concentration of mixtures, but also by the surface interactions or application of the electric field. They also reported the observation of the thresholdless switching in the mixture, too.

Though a real example of the intrinsic thresholdless antiferroelectric V-shaped switching has not been found so far, research in thresholdless antiferroelectricity actually has led to a discovery of ferroelectric V-shaped switching, which is still important for applications and for advancing scientific understanding. Additionally it has also motivated the discovery of the so-called frustration phenomenon that was observed in binary mixtures by Gorecka *et al.* [35,36]. In particular, the frustration phenomenon is still unclear in both its characteristics and mechanism. Furthermore, frustration has much similarity with thresholdless switching. The main purpose of this paper is to clarify the so-called frustration phenomenon using mixtures of antiferroelectric MC881 and ferroelectric MC452 compounds, which were originally synthesized for the development of the thresholdless antiferroelectricity by MGC. We investigate the mechanism and the origin for the frustration phenomenon, clarifying the effects of the mixing ratio, the surface confinement, and the applied field. We also reexamine the two mechanisms already suggested for thresholdless antiferroelectricity: that is, the continuous evolution of ϕ and the Langevin-like alignment. These investigations are carried out in view of the consideration that the interlayer interaction energy can provide answers for the various questions regarding the frustration phenomenon and thresholdless antiferroelectricity. Finally, we also report clear experimental results supporting ferroelectric V-shaped switching using the MGC compounds, nominally optically pure R-moiety MC452 and S-moiety MC536.

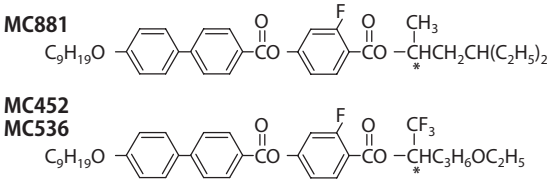

FIG. 1. Chemical structures of antiferroelectric MC881 and ferroelectric MC452, which show simple phase sequences: I (122 °C) SmA^* (114.5 °C) SmC_A^* and I (107.2 °C) SmC^*, respectively. Both MC881 and MC452 are R-moieties. MC536 is the S moiety of MC452.

II. EXPERIMENT

The samples used are the binary mixtures of antiferroelectric MC881 and ferroelectric MC452 compounds with chemical structures shown in Fig. 1. These were synthesized by MGC and are the so-called "V-shaped switching materials" for gray-scale displays [19–21]. In these references some of the mixtures as well as MC452 were considered as *ferrielectric*, since the melatopes in conoscopy emerged parallel to the applied electric field. As was already pointed out in Sec. I, Song *et al.* have nevertheless unambiguously identified them as ferroelectric [22]. Both homeotropically and homogeneously aligned cells of these samples were prepared using a Dow Corning silane coupling agent, 72% 3-(trimethoxysilyl)propyldimethyloctadecyl ammonium chloride and 28% methanol, and a Nissan Chemical aligning agent, RN1175, respectively. Various cells ranging in thickness from less than 1 μm and up to 100 μm were used for carrying out the following experiments, which are essential for advancing the subject.

We first obtain the bulk phase diagram in the MC881-MC452 binary-mixture system using sufficiently thick cells. Phase boundaries are determined by monitoring the dielectric response in terms of measuring the real part of the dielectric permittivity, spectroscopic Bragg reflection, and electric-field-induced birefringence. The latter is investigated using a photoelastic modulator (PEM) setup. The dielectric measurements are carried out at a frequency of 1 kHz with an impedance analyzer (HP-4192A) using 25-μm homogeneous (planar) cells. As was actually used in the phase identification of a prototype antiferroelectric liquid-crystal compound, MHPOBC [37], the soft mode in SmA and the Goldstone mode in SmC^* are used for determining the phase transition temperatures among isotropic SmA, SmC^*, and SmC_A^* by observing the low-frequency dielectric permittivity. The Bragg reflection bands of 100-μm homeotropic cells are also measured at an oblique incidence angle of 20° using a UV-visible-IR spectrophotometer (Perkin Elmer, Lambda 900). As is generally known now, SmC^* has the full-pitch helical periodicity and hence shows not only the characteristic reflection band (half-pitch band), but also the full-pitch band, whereas SmC_A^* with the half-pitch helical periodicity only gives the characteristic reflection band [1]. Since both the dielectric and spectroscopic measurements show some complexities, which in turn suggest the emergence of subphases between SmC^* and SmC_A^*, the electric-field-induced birefringence of 25-μm homeotropic cells has been investigated for

determining the electric-field-temperature (E-T) phase diagram by using an experimental setup using a PEM. Our previous papers [38,39] give a detailed description of the PEM-based setup for measuring the electric-field-induced birefringence using homeotropic cells together with the effectiveness of such results in identifying the subphases.

For a better observation of the frustration phenomenon, we studied the interface-induced destruction of the anticlinic antiferroelectric order in SmC_A^* by using sufficiently thin homogeneous cells. Phase boundaries were determined by analyzing the data on the real part of the dielectric permittivity measured at 1 kHz with the same apparatus as described above. Particular attention was paid to the thermal hysteresis effects, since the boundary critically depends not only on the cell thickness used, but also on the cooling and heating processes. We also investigated the switching characteristics by using 9-μm cells of several mixtures at 35 °C, one of which was clearly located in the SmC_A^* region in the bulk phase diagram obtained above and exhibited a similar behavior to so-called V-shaped switching. Polarized Raman scattering was measured using a 2-μm cell during switching as well as without an applied field. The experimental setup and the analysis for Raman scattering data followed the methods suggested by Hayashi *et al.* [40,41]. In order to clarify the cause of the emergence of a thresholdless response to the applied electric field in SmC^*, we observed the texture of 1-μm cells of MC452 (R-moiety) and its partially racemized mixture with MC536 (S-moiety) using a optical polarizing microscope (Olympus BX-52).

Then we tried to determine experimentally the free-energy plot against the azimuthal angle difference between the adjacent smectic layers for the various data points (specified by the concentration and temperature) in the SmC_A^* region of the above-obtained binary-mixture phase diagram. By assuming the uniaxial distribution of the molecular short axes as well as the perfect orientational and translational order, the free energy at a particular temperature can be written in a very simplified form as

$$F = \text{const} + D\cos\phi - Q\cos 2\phi - P_s E\cos\phi, \tag{1}$$

where ϕ is the azimuthal angle difference of the in-layer directors between the adjacent layers and const, D, and Q are functions of the director tilt angle, and P_s is the spontaneous polarization [42–44]. The coefficients D and Q are given as functions of experimentally measurable quantities [13,45,46]:

$$D = \frac{3\cos(\phi_{\text{th}}/2)+2}{4\{\cos(\phi_{\text{th}}/2)+1\}^2} P_s E_{\text{th}}, \tag{2}$$

$$Q = \frac{1}{16\cos(\phi_{\text{th}}/2)\{\cos(\phi_{\text{th}}/2)+1\}^2} P_s E_{\text{th}}. \tag{3}$$

Here E_{th} is the critical field and ϕ_{th} indicates the value of ϕ at $E=E_{\text{th}}$. The critical field E_{th} can be determined as a field where the solitary wave observed during the field-induced switching from SmC_A^* to SmC^* has zero speed [13,45]. We can also determine $\phi_{\text{th}} = \pi - 2\sin^{-1}(\tan\Theta'/\tan\Theta)$ by measuring the apparent tilt angle Θ' at E_{th} and the director tilt angle Θ in the field-induced SmC^*. The free-energy difference Δ and the barrier height H between the SmC_A^* and SmC^* minima are calculated using Eq. (1):

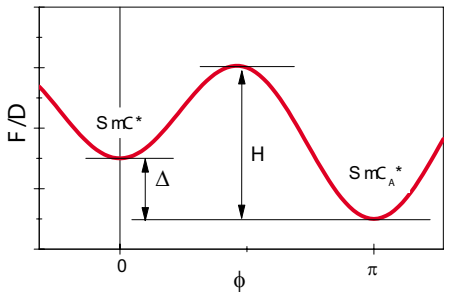

FIG. 2. (Color online) The interlayer interaction energy divided by the coefficient of dipolar term represented by Eq. (1) when $Q/D=2$ as a function of the angle beteen the two neighboring layers.

$$\Delta = 2D, \quad H = \frac{D^2}{8Q} + 2Q + |D|. \tag{4}$$

Figure 2 illustrates the free energy having the dipolar and the qudrupolar terms.

III. RESULTS AND DISCUSSION

A. Phase diagram of the MC881-MC452 binary-mixture system and the gradual phase transition

Figure 3 shows the temperature-concentration (T-x) phase diagram in the binary-mixture system of anticlinic antiferroelectric MC881 and synclinic ferroelectric MC452. In order to be free from any interface effects, the phase diagram was obtained using 25–100-μm-thick cells. The phase boundary neither depends on the cell thickness nor shows obvious thermal hysteresis, so far, by using such thick cells. The bound-

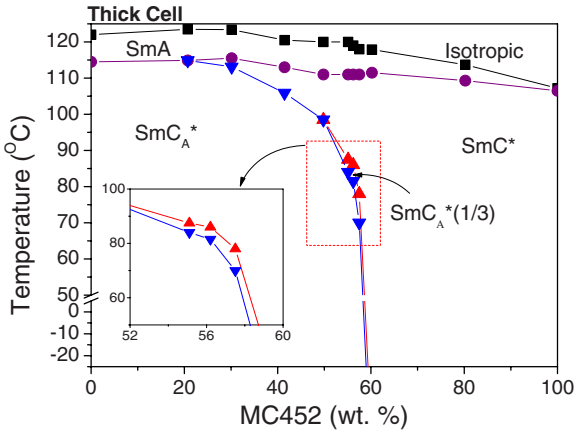

FIG. 3. (Color online) Bulk phase diagram of a binary-mixture system of MC881-MC452 using thick cells varying in thickness from 25 to 100 μm. The boundary between SmC_A^* and SmC^* becomes almost vertical and runs parallel to the ordinate temperature axis below 70 °C, so that we can define the critical concentration R_c as roughly 59% of MC452. The mixture near R_c stably exists as smectics even at −25 °C.

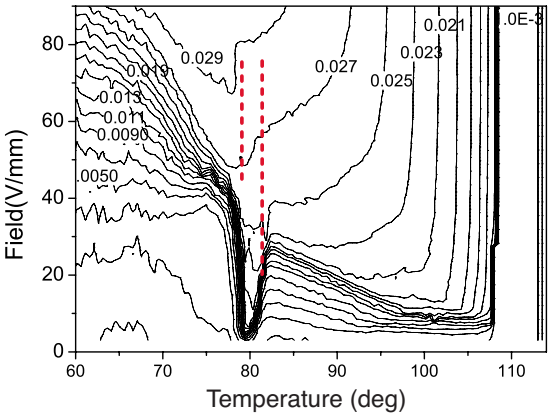

FIG. 4. (Color online) PEM data, indicating clearly the emergence of subphase $SmC_A^*(1/3)$. The red dotted lines indicate the transitions between SmC_A^* and $SmC_A^*(1/3)$ and between $SmC_A^*(1/3)$ and SmC^*. The concentration of MC452 in the mixture is 56.2 wt. % as for the rectangle shown in the inset of Fig. 3.

ary between SmC_A^* and SmC^* is almost vertical and parallel to the temperature axis in the low-temperature region from ca. 70 °C down to at least −25 °C as contrasted with the ordinary one which slants significantly [47]. In the molecular theory for anticlinic SmC_A [43], SmC_A^* always becomes stable at low temperatures, and there should exist SmC_A^* at sufficiently low temperatures if the compound does not directly reach any other lower-temperature liquid-crystalline or crystalline phase. Figure 3 clearly indicates that SmC_A^* could not exist as a low-temperature phase of SmC^* on the right side of the vertical boundary. This means that there exist some intermolecular interactions that absolutely stabilize SmC^* by surpassing the ones which usually produce SmC_A^* at low temperatures. Such intermolecular interactions may also be responsible for the appearance of reentrant SmC^* reported by Pociecha *et al.* [48]. We shall designate the mixing ratio corresponding to the vertical line as the critical concentration $R_c \approx 59\%$. The $SmC_A^*(1/3)$ phase having three-layer periodicity was observed over a narrow range of temperatures at the boundary. The existence of $SmC_A^*(1/3)$ can be confirmed by PEM results shown in Fig. 4.

A second phase diagram was constructed by using dielectric permittivity measurements on thinner cells of 2-μm thickness. The experiments were carried out during both heating and cooling cycles. The obtained phase diagram is shown in Fig. 5. Since the dielectric permittivity changes gradually in thin cells especially near the critical concentration $R_c \approx 59\%$, it is not easy to directly determine the exact transition temperature, but we defined it to correspond to the center of the gradually changing dielectric permittivity. In thin cells, the SmC^*-SmC_A^* transition temperatures obtained during cooling are much lower than those during heating; that is, the supercooling effect is significantly large. It is so large near R_c that the transition is not detected during the cooling cycle at all. Since the supercooling is not observed in the thick cells, we can conclude that the supercooling in thin cells basically arises from the surface effects, but its mechanism has not been explained clearly so far. Figure 6 shows the real part of the dielectric permittivity as a function of

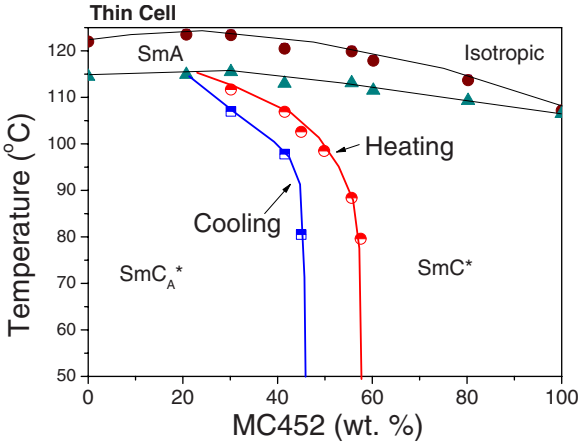

FIG. 5. (Color online) Phase diagram obtained by dielectric permittivity measurements in 2-μm thin cells.

temperature in two thick cells and one thin cell for 40 and 55.5 wt. % MC452 mixtures in MC881. For 40 wt. % MC452 mixture in a thick cell, the SmC^*-SmC_A^* transition is clearly detected in a narrow range of temperatures, which is the common behavior observed for the phase transition. However, the transition is rather dull and unclear in the thin cell using the same mixture or in the thick cell using the 55.5 wt. % MC452 mixture. The dull curves of the real part of dielectric permittivity clearly show that the phase transition occurs gradually over a wide range of temperatures. The confinement by surfaces and the concentration of the binary mixtures result in the same effect at the phase transition—that is, the transition occurs gradually—as was already reported by Gorecka *et al.* [35,36].

In order to find the origin of the gradual phase transition, we carried out yet another experiment as shown by results in Fig. 7, where the two sets of the real part of the dielectric permittivity are plotted using the same cell with different thermal histories. The dielectric permittivity was measured using a 2-μm-thick planar cell of 50 wt. % MC452 mixture at a frequency of 1 kHz. After filling the cell with the 50 wt. % mixture at its isotropic temperature, the cell was

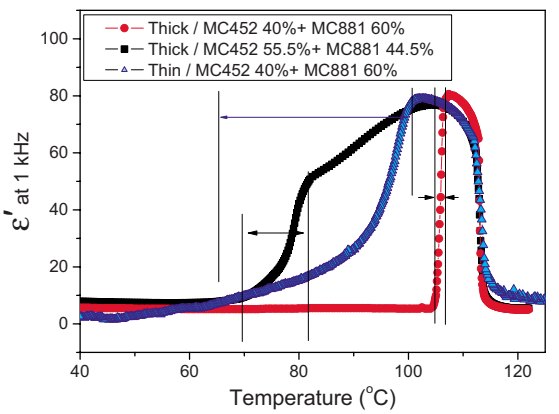

FIG. 6. (Color online) Real part of dielectric permittivity measured at 1 kHz using various cell conditions. The cell conditions are given in the inset: "thin" and "thick" indicate about 2-μm and 25-μm thin cells, respectively. Cooling rate is −0.2 °C per min.

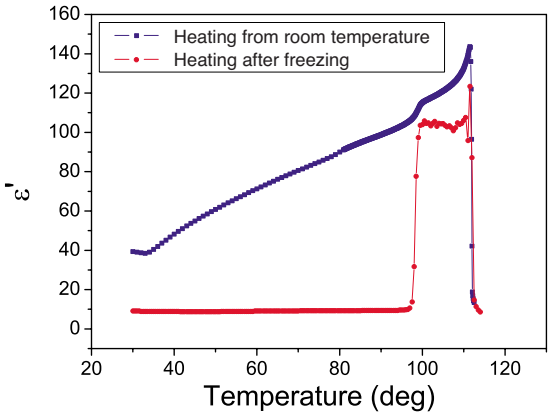

FIG. 7. (Color online) Real part of dielectric permittivity measured at a frequency of 1 kHz using a 2-μm thin cell of 50 wt. % MC452 mixture. Blue square data points were obtained during heating the cell after keeping at room temperature for 5 h, and red circle data points were obtained during heating the cell after keeping at −5 °C for 2 h. The heating rate is 0.3 °C/min.

cooled down to room temperature. First, the blue square data points were obtained during heating from room temperature. For the second experiment, the cell was cooled down again to −5 °C and was kept for 2 h. Then, the red circle data points were obtained during heating. A clear difference is detected as shown in Fig. 7. The cell kept at −5 °C shows a sharp step near 98 °C, which indicates a clear phase transition from SmC_A^* to SmC^*. However, for the other cell kept at room temperature, the transition is unclear. The dielectric response for the cell kept at −5 °C is the typical behavior for the SmC_A^*-SmC^* phase transition. The dielectric response for the cell kept at room temperature is rather close to that of SmC^* except for a slight jump in ϵ' close to the transition temperature. This implies that the liquid crystal at room temperature is not in a completely synclinic or in an anticlinic state, but this is a mixture involving both the synclinic and anticlinic states. On heating from room temperature, only a part of the cell experiences the phase transition at the transition temperature, since the other part is already in SmC^*. By keeping the cell at a low temperature, the partially synclinic state changes completely into the anticlinic state, and the liquid crystal acquires pure SmC_A^*. Therefore, in the area between the two vertical transition lines in the phase diagram shown in Fig. 5, the two phases can obviously coexist simultaneously.

Gorecka *et al.* [35,36] explained these phenomena as the frustration between the antiferroelectric and ferroelectric phases and the formation of nanosize (smaller than visible wavelength) antiferro- and ferroelectric clusters. In order to support their model, they introduced the interlayer interaction between the neighboring layers as a simple term $f_i = A_1(\xi_i \cdot \xi_{i+1})$ by neglecting higher terms, where ξ_i represents the director vector of ith layer. This interlayer interaction energy can simply be represented as $f_i = A_1' \cos\phi$, which is the dipolar term in Eq. (1). Hence, when mixing with an appropriate ratio the antiferroelectric and ferroelectric liquid-crystalline materials, the coefficient A_1' proportional to A_1 approaches zero and the interlayer interaction energy becomes independent of ϕ. They pointed out that this weak ϕ correlation of the interlayer interaction is the origin of the frustration and the formation of the clusters. However, the quadrupolar term in the interlayer interaction in the antiferroelectric phase has widely been reported to exist and is known to play an important role in the switching of the antiferroelectric phase and the phase transition to occur. Qian and Taylor [12] showed that the quadrupolar term actually determines the switching characteristics of an antiferroelectric cell, and Song *et al.* [42,45] showed that the quadrupolar term prohibits the homogeneous phase transition and instead makes it possible for solitary-wave propagation to occur. Solitary-wave propagation leads to a slow nonhomogeneous process and is quite different from a homogeneous phase transition. Therefore, it is impossible to understand the phase transition appropriately without the quadrupolar term as was attempted by Gorecka *et al.* [35,36].

B. Thresholdless antiferroelectric switching in the binary mixture

Though the effects of applying an electric field on antiferroelectric cells are apparently different from those of applying thermal energy, the electric-field-induced switching behavior quite resembles the temperature-induced phase transition. This is because the electric field favors and induces the ferroelectric state as does the thermal energy. Note that the thresholdless switching with field is very similar to the gradual phase transition with temperature. Hence, investigating field-induced continuous switching is quite helpful in understanding the temperature-induced gradual phase transition.

We measured the apparent tilt angle Θ' as a function of the applied field using 9-μm cells. Figure 8 shows the field dependence of the apparent tilt angle for the various mixing ratios. The experiments were carried out with both increasing and decreasing electric fields at 35 °C using 9-μm planar cells. As the concentration of MC452 increases, the threshold field for the antiferroelectric-ferroelectric (AF-F) transition decreases, while the AF-F switching for a 30 wt. % MC452 mixture shows a clear one-step increase. This is a typical behavior of antiferroelectric materials; the AF-F switching for the mixtures with higher concentrations of MC452 shows a two-step increase and finally leads to a rather gradual increase as shown in Fig. 8. To identify the intermediate state at the two-step switching, we simulate the apparent tilt angle in the SmC_A^*(1/3) structure shown in Fig. 9. The tilt angle Θ for the 40 wt. % mixture at 35 °C is 37°. For $\Theta = 37°$, $n_o = 1.5$, and $n_e = 1.7$, the apparent tilt angle Θ' for the unwound SmC_A^*(1/3) state is found to be 30.4° in our calculations, which is the same as Θ' found experimentally in the intermediate state. This implies that the intermediate state is the field-induced SmC_A^*(1/3) state. This indicates that the field plays almost a similar role to that played by the thermal energy. Note that SmC_A^*(1/3) was observed between SmC^* and SmC_A^* in the phase sequence with temperature as shown in Figs. 3 and 4. Similarly, the SmC_A^*(1/3) state is observed in the intermediate range of fields between the antiferroelectric and field-induced ferroelectric states [51–53]. As the

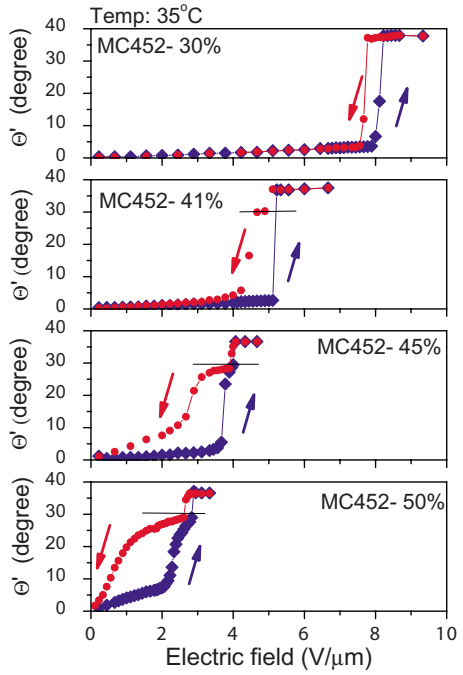

FIG. 8. (Color online) Apparent tilt angle Θ' as a function of the applied field measured at 35 °C using 9-μm cells of MC881 mixtures containing various wt . % of MC452. Each measurement is carried out with increasing or decreasing field as indicated by an arrow. Black thin horizontal line in each of 41 wt. %, 45 wt. %, and 51 wt. % shows the simulated state for the three-layer structure. For 41 wt. % composition the two-step decrease is observed only during the field decreasing, whereas for 45 and 50 wt. % the two-step process is observed during both the field increasing and decreasing.

concentration of MC452 increases, the range of $\mathrm{SmC}_A^*(1/3)$ is enlarged. An almost gradual increase in the apparent tilt angle is observed as the mixing ratio approaches the critical concentration R_c, but still it shows the two-step increase.

The $\mathrm{SmC}_A^*(1/3)$ phase is not observed in thin cells. This may be because the stability of $\mathrm{SmC}_A^*(1/3)$ is rather weak and is easily suppressed by the surface energy. Similarly, a thinner cell may show a better continuous switching without the two step increase. We prepared thin 2-μm cells of 55 and 45 wt. % MC452 mixtures; the 55 wt. % mixing ratio is close to the critical concentration ($R_c \approx 59$ wt. %). In order

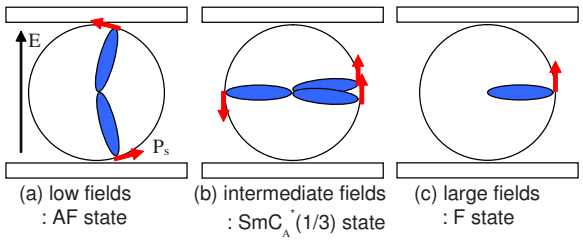

FIG. 9. (Color online) The relative orientation of the c directors at each step of the field induced transition. When $\Theta = 37°$, $n_o = 1.5$, and $n_e = 1.7$, $\Theta' = 30.4°$ is found for the $\mathrm{SmC}_A^*(1/3)$ state according to a simple simulation. The simulation result accords well with the experimental results shown in Fig. 8; see the horizontal thin black lines.

to make sure that all the material in the cell becomes $\mathrm{Sm}C_A^*$, the cells were kept at a temperature of −5 °C for 15 h. After heating the cell to room temperature, the apparent polarization was measured by increasing and decreasing the applied field as shown in Fig. 10. Three sets of measurements were carried out for each cell: the first data were obtained in the virgin cell with increasing field; then, the second data were obtained with decreasing field and the third ones obtained with increasing field again.

The 45 wt. % MC452 cell [Fig. 10(b)] shows a threshold field, which is the typical behavior of the antiferroelectric phase. The third data correspond similarly to the first one, which means that the field-induced ferroelectric state easily returns to the initial antiferroelectric state when the field is removed. On the other hand, the 55 wt. % MC452 cell [Fig. 10(a)] shows a gradual increase in the polarization with increasing field, which is quite similar to the thresholdless antiferroelectric behavior. Since the virgin cell is in SmC_A^*, continuous switching means that the antiferroelectric phase gradually transforms to the field-induced ferroelectric state. However, the third set of data are similar to the second data set, but are different from the first one. This means that the field-induced ferroelectric state does not return to the initial antiferroelectric state after removing the field. Hence, the third data represent the switching of a ferroelectric cell, which means that the thresholdless antiferroelectricity is possible only for the first switching. After all, the thresholdless antiferroelectricity is possible as shown in Fig. 10(a), although the behavior is rather different from the conventional concept of thresholdless antiferroelectric switching, because conventional switching is supposed to be used in applications and should occur at high frequencies as well; that is, the antiferroelectricity should recover quickly when turning the applied field off. Hence, the kind of thresholdless antiferroelectricity observed here is not useful for applications.

C. Mechanism of the frustration and the solitary waves

As pointed out by Qian and Talyor [12] and later by Parry-Jones and Elston [13], the interlayer interaction is the most crucial factor in determining the characteristics of the phase transition between the $\mathrm{Sm}C_A^*$ and $\mathrm{Sm}C^*$. Now, we will reexamine the two models suggested for the thresholdless antiferroelectric switching mode: the continuous evolution model and the Langevin-like model from the viewpoint of the interlayer interaction energy. Based on the electrostatic dipolar interactions, Lee and Lee presented a geometrical model for the change in the azimuthal angle and gave the thresholdless criterion [10]. Qian and Talyor and more recently Parry-Jones and Elston made a detailed analysis of the change in terms of the interlayer interaction energy as a function of the azimuthal angle difference between the adjacent layers at any given applied electric field [12,13]. Continuous evolution can be achieved when the quadrupolar term is small enough as compared with the dipolar term and the interlayer interaction has always one energy minimum. Figure 11 shows the free energy plotted against ϕ for various values of the applied fields for three parametric values of

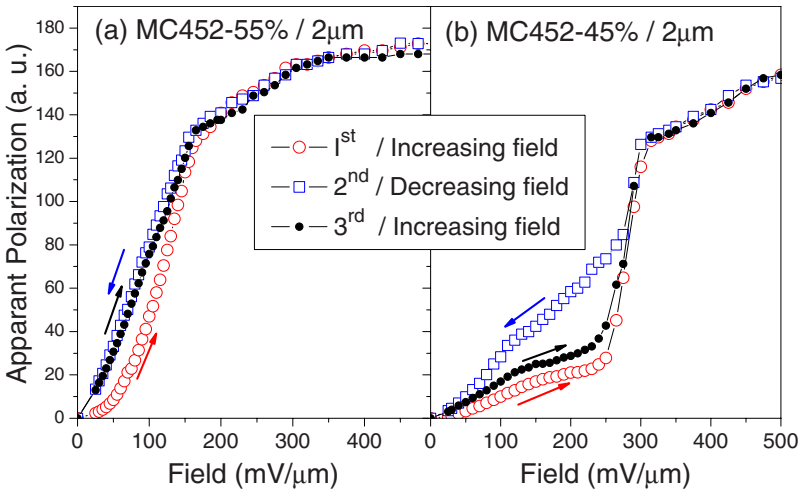

FIG. 10. (Color online) Apparent polarization as a function of applied field in 2-μm cells of MC881 mixtures containing (a) 55 wt. % and (b) 45 wt. % MC452.

Q/D. When Q/D is large enough as shown in (c), the free energies have two energy minima at various applied fields, and tristable switching is expected. However, when the quadrupolar term is very weak as shown in (a) ($Q/D \leqslant 0.05$), the free-energy plots have always a single energy minimum, and continuous evolution is expected.

Therefore, if there exists such a material having a very weak quadrupolar interlayer interaction term as compared to the dipolar term, continuous evolution—that is, thresholdless antiferroelectricity—can be obtained even in a thick cell. However, all of the thresholdless switchings in AFLC cells have so far been obtained in a thin cell only, and most of these have been revealed as ferroelectric V-shaped switchings since the surface suppresses the antiferroelectricity as shown in the previous section. In molecular theories, synclinic ordering is favored by the isotropic dispersion attraction between the molecules and the steric energy between the layers, which are supposed to be the most dominant interlayer interaction energies [43]. Therefore, the existence of the local minimum at the synclinic ordering is naturally expected even in the antiferroelectric phase, which also supports the presence of a significantly large quadrupolar term, as is being actually obtained in the following. In this way, though continuous evolution is possible theoretically, an actual material having such physical properties may not exist. Langevin-like alignment assumes a ϕ-independent free energy and a randomized angle difference between the adjacent layers. This may be possible only when both the dipolar and quadrupolar terms are close to zero. Using the same reasoning as given above, liquid-crystalline material having a weak tilting direction correlation is also difficult to realize.

We measured the actual interlayer interaction energy in the binary mixtures using the method explained in Sec. II. Figure 12 shows the data for measured H, Δ, and Q/D plotted as a function of temperature in 25-μm planar cells of the binary-mixture system of MC881-MC452. We can see that Q/D is always much larger than 0.25, which means that there exist always two energy minima. While H does not change much with the mixing ratio, Δ decreases with increasing MC452 concentration. Note that Δ and H represent the energy difference and the barrier height between the two energy minima, respectively. Each of the minima represents the stable state of a phase. Therefore, the large value of H implies that there exists the large energy barrier between the two phases. The trend of Δ with the concentration is quite interesting. The average values of Δ over the temperature range from (T_c-50) °C to (T_c-10) °C are plotted as a function of the concentration in Fig. 13. $\langle\Delta\rangle$ approaches zero at R_c, which means that the energy difference between the anticlinic and synclinic orderings becomes zero as the concentration approaches the critical concentration. This experimental observation is quite understandable. Pure MC881, which is an antiferroelectic material, has the minimum free-energy level in anticlinic ordering. By adding MC452, which is a ferroelectric material, the free-energy level in synclinic ordering decreases and consequently Δ decreases. Since the synclinic and anticlinic orderings have the same energy level close to the critical concentration R_c, Δ reduces to zero. Hence, we can conclude that by adding the ferroelectric material to the antiferroelectric one, the energy difference between the synclinic and anticlinic orders is reduced, but the energy barrier between these two states is little influenced.

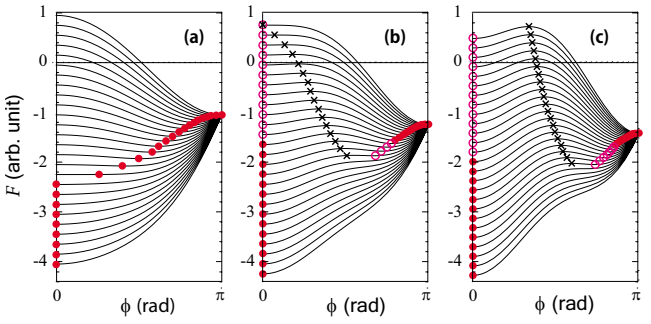

FIG. 11. (Color online) Free energy as a function of the azimuthal angle difference of the in-layer directors between the adjacent layers for various strengths of an applied electric field calculated using Eq. (1). The values of parameters: (a) $Q/D=0.05$, (b) $Q/D=0.25$, and (c) $Q/D=0.5$. The applied field increases from top ($E=0$) to bottom curve for each graph. Solid red circles are global minimum points, open pink circles are local minimum points, and brown crosses are the energy barrier between the two energy minima. For $Q/D \leqslant 0.05$, only a single minimum exists at any applied electric field, and for $Q/D > 0.25$, $\phi=0$ is the local energy minimum even at zero field.

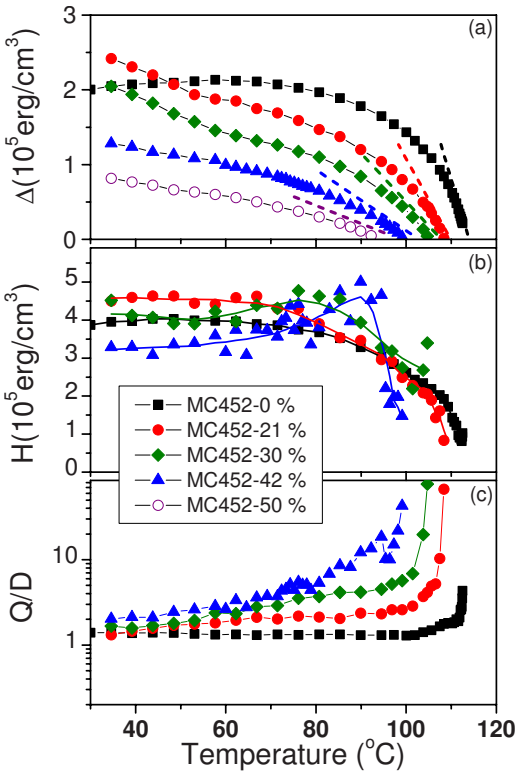

FIG. 12. (Color online) (a) Free-energy difference between SmC_A^* and SmC^* minima, (b) its barrier height separating these, and (c) Q/D with temperature. The results are obtained through solitary-wave experiments using 25-μm thick planar cells.

Moreover, the slope of Δ with temperature depends on the concentration. The dotted line for each curve represents the slope of the curve near T_c in Fig. 12(a). The absolute values of the slope of the lines are plotted in Fig. 13, which show that the slope also approaches zero as the mixing ratio gets closer to R_c.

Actually, we can explain the gradual phase transition phenomenon using the above-measured interlayer interaction energies. In our previous paper [45], we showed that, when there exists an energy barrier between the ferroelectric and antiferroelectric energy minima as in the binary mixtures under consideration, the only possible way for the phase transition to occur is a nonhomogeneous process—i.e., solitary-wave propagation—to overcome the energy barrier [42,45]. Usually, the solitary wave starts from defects and its propagation is also influenced by surface effects. The energy difference between the two phases, Δ, is the driving force for the solitary wave to propagate. Therefore, the phase transition depends strongly on the competition between the driving force controlled by Δ, on the one hand, and the frictional effect controlled by surfaces on the other and the presence of defects. When Δ is large, the driving force for the phase transition is so strong that the transition occurs very quickly. On the other hand, if Δ is small, the driving force is weak compared to the friction. While in some parts of the cell, the transition may successfully occur slowly, but in the other part, the metastable state would remain and the two phases may actually coexist. This explains why the coexistence of two phases appears close to the critical concentration R_c,

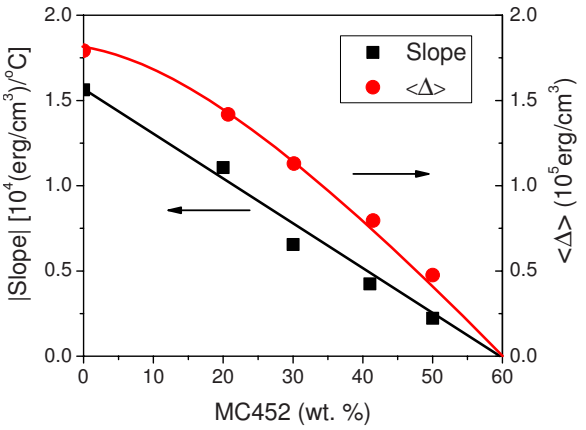

FIG. 13. (Color online) Averaged $\langle\Delta\rangle$ over the temperature range from (T_c-50) °C to (T_c-10) °C (upper) and the absolute value of the slope near T_c (lower) as a function of wt. % of MC452 in MC881.

where the energy difference Δ is minimized as shown in Figs. 12 and 13. The slope of Δ with temperature is the most important factor. As shown in Fig. 13, the slope approaches zero near the critical concentration. The low value of the slope means that Δ becomes weakly dependent on the temperature. On cooling, Δ experiences its sign reversal at the transition temperature T_c, and the anticlinic ordering, which was the metastable state at high temperatures, becomes the global stable state. On further cooling, Δ increases and the driving force for solitary-wave propagation increases. If the slope of Δ is large as for the case for a large concentration of MC881, Δ increases quickly with decreasing temperature and the phase transition occurs rapidly in a narrow range of temperatures. However, if the slope of Δ is small as being near the critical concentration, Δ increases very slowly with decreasing temperature and the driving force for the solitary wave to propagate is rather weak, even when the temperature is much lower than T_c. Hence, large supercooling and at the same time rather dull phase transitions are observed as shown in Figs. 5 and 6. The slope of Δ explains why the phase transition line between the SmC_A^* and SmC^* phases in the phase diagram is vertical. The slope approaches zero at R_c: the zero slope means that the transition between SmC^* and SmC_A^* occurs almost at the same concentration over a wide range of temperatures, and the transition line in the phase diagram becomes vertical. The thresholdless antiferroelectricity shown in Fig. 10(a) is similarly explained. Furthermore, the reason as to why the antiferroelectricity does not recover after removing the field is explained by the fact that Δ is small and the driving force for the solitary wave is too weak for the propagation to occur.

D. Possible ferroelectric V-shaped switching in very thin cells of bulk antiferroelectric mixtures with nearly critical concentrations

In this way, the coexistence of the SmC_A^* and SmC^* phases over a wide range of temperatures is explained by the suppression of the solitary waves. So far, the various phe-

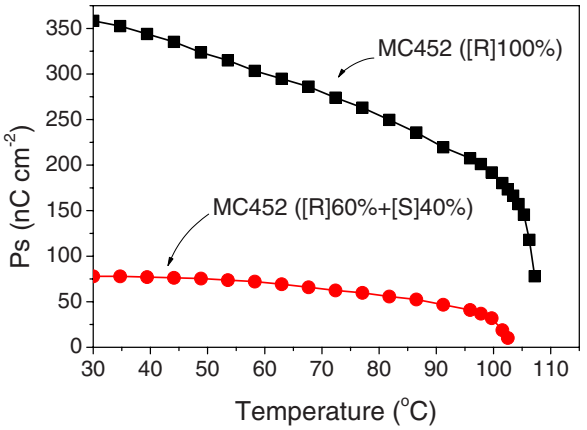

FIG. 14. (Color online) Spontaneous polarization of nominally optically pure *R*-moiety MC452 and its partially racemized mixture of enantiomeric excess, e.e.$=([R]-[S])/([R]+[S])=0.20$, with the *S*-moiety of MC452 (i.e., MC536).

nomenological theories regarding the SmC_A^*-SmC^* transition have been suggested, but these models deal with only the static free-energy minimum, but not the dynamic process of the phase transition. These models have provided valuable information for finding the phase having the minimized free energy at a given temperature and in finding the phase sequence with temperature, but these are not applicable to explaining how the phase transition occurs at the transition temperature. This is why it has widely been believed that the phase transition may simply occur when the minimum free energy shifts from one phase to another phase. However, our investigation of the dynamic process of the phase transition clearly shows that the transition is not simple and the process can be easily suppressed. The terminology "frustration" seemed to be chosen due to the belief that the transition may rather simply occur, and as a result, the coexistence of the two phases is regarded as the frustration state, which means both phases can be excited thermally and these can easily be transformed to each other due to a small energy difference between the two phases. However, as explained above, the coexistence of the two phases is actually caused by the suppression of the phase transition. The suppression is more effective when the energy difference between the two phases is small and the friction by the surfaces is strong; hence, the coexistence and the gradual transition appear close to the intermediate concentration and furthermore in a thin cell. Thus, the gradual phase transition or the so-called frustration phenomenon can be explained clearly by the suppression mechanism.

When the cell becomes really thin—e.g., 1 μm or less in thickness—so that the surface effects favoring ferroelectricity prevail in the entire sample, the surface-stabilized ferroelectric states, in particular, the twisted ones, may possibly be produced even in the bulk antiferroelectric mixtures. This is particularly easy to occur when the mixture concentration is close to the critical one R_c. Note that the surfaces are more or less polar and force the spontaneous polarization in each layer to direct outwards or inwards. Depending on the polarity of the surfaces and the sign of the spontaneous polarization of the sample mixture smectics, there exist two kinds of twisted states: TR1 and TR2 or TL1 and TL2 [49]. When the spontaneous polarization is large, an elastic constant concerning the **c**-director bend deformation apparently becomes very large because of the considerable bulk polarization charges, $\rho_P=-\mathrm{div}\mathbf{P}_s$, caused by the deformation [23,24]. Therefore, the directors tend to be parallel to each other in planes vertical to the substrate plates to avoid any deformed structure so that the twisted regions become extremely thin and finally diminish; consequently, the complete extinction direction of the cell is observed along the smectic layer normal as contrasted with the ordinary twisted states. Mottram and Elston [14,15] reported a detailed theoretical investigation into the effects of polar anchoring, which induces ferroelectric ordering close to the cell surfaces, in a liquid-crystal cell containing an antiferroelectric liquid-crystalline material. Experimentally, in fact, the V-shaped switching is almost observed in a 2-μm cell of the binary mixture with a concentration of MC452 close to R_c as shown in Fig. 10.

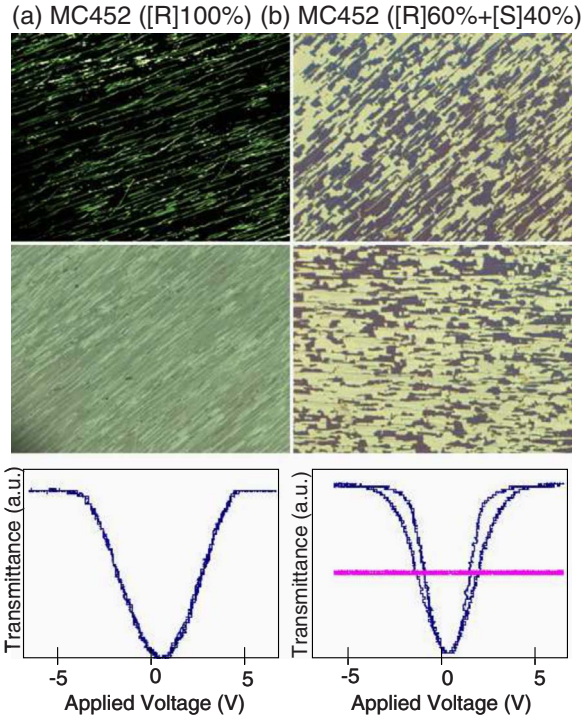

FIG. 15. (Color online) Nominally optically pure *R*-moiety MC452 (e.e.$=1$) shows a single domain with its extinguishing direction parallel to the smectic layer normal in a cell of thickness about 1 μm (a), while its partially racemised mixture with *S*-moiety MC536 has two domains (b). The switching characteristic abserved at 0.1 Hz triangular wave also shows the difference. The pink horizontal line in the switching graph (b) is the optical transmittance when the applied field is turned off; this is due to the presence of domains.

Although we have not yet performed any detailed switching experiment near the critical concentration region, we have observed ferroelectric V-shaped switching in the ferroelectric component of the binary mixture system here studied, MC452. Here we show the rather direct evidence for the relation between the switching characteristics and the polar-

TABLE I. Apparent order parameters obtained for pure MC452 at 25 °C by polarized Raman scattering. The apparent tilt angle is 37.9° and deporalization ratio is 0.367.

Measuring condition	Observed $\langle P_2 \rangle$	Observed $\langle P_4 \rangle$
Applied electric field (±25 V)	0.890	0.700
No applied field (0 V)	0.721	0.331
At the tip of the V[a]	0.803	0.459

[a]$\langle P_2 \rangle$ and $\langle P_4 \rangle$ were obtained by applying a 0.1-Hz triangular field. The tip of the V implies zero field during the switching experiment.

ization. We used nominally optically pure MC452 and a partially racemized R (MC452) and S (MC536) mixture of enantiomeric excess, e.e.$=([R]-[S])/([R]+[S])=0.20$ or 60 wt. % of MC452. The racemized mixture has about 20% of the maximum polarization of the optically pure material as seen in Fig. 14. The sign of polarization in MC452 is negative. The textures observed under crossed polarizers are given in Fig. 15. The pure MC452 cell shows a single domain, the extinction direction of which is along the smectic layer normal, whereas the e.e.$=0.20$ or the cell with 60 wt. % of MC452 shows two domains, which are the twisted-surface-stabilized states TL1 and TL2. The substrate surfaces coated with RN-1175 apparently force the spontaneous polarization vectors to point outward. The lower part of Fig. 15 illustrates the response to a 0.1-Hz triangular waveform electric field. It is of excellent V-shaped switching character and becomes sufficiently dark at $E=0$ in the pure MC452 cell. When the field is turned off, it still becomes dark. On the other hand, the e.e.$=0.20$, i.e., for MC452 60 wt. % cell does not become sufficiently dark at $E=0$ and shows some hysteresis; when the field is turned off, it is naturally not dark, for there exist the two domains.

To confirm the vertical steep alignment of the in-plane directors, responsible for the single domain and the nice V-shaped switching observed, we obtained the apparent order parameters $\langle P_2 \rangle$ and $\langle P_4 \rangle$ by polarized Raman scattering and compared them with the calculated ones with various standard deviations σ's [54]. Results are summarized in Tables I and II. The in-plane directors are apparently aligned parallel to the plane normal to the smectic layer and vertical to the substrate plates, although the standard deviation is rather large $\sigma=17.5°$, since our cell preparation technology was not good as seen in Fig. 15. The distribution becomes sharper at the tip of the V, as has been noticed in the early stages of investigation [50]. Similar experimental investigations in the antiferroelectric binary mixtures near the critical concentration R_c are interesting future problems to be studied.

IV. CONCLUSIONS

We have investigated the gradual phase transition observed in binary mixtures of MC881 with several MC452 concentrations. These materials were originally synthesized for obtaining the thresholdless antiferroelectricity for use in displays. The similar phenomenon of gradual phase transition was reported by Gorecka *et al.* for the first time, but it

TABLE II. Calculated order parameters $\langle P_2 \rangle$ and $\langle P_4 \rangle$ for pure MC452.

Assumed σ (deg)	Calculated $\langle P_2 \rangle$	Calculated $\langle P_4 \rangle$
0.1	0.828	0.570
7.5	0.815	0.539
10	0.792	0.485
12.5	0.770	0.436
15	0.746	0.387
17.5	0.720	0.335
20	0.692	0.284

was not clearly clarified mostly due to a poor understanding prevailing at the time about the interlayer interactions and in particular by their neglect of the quadrupolar term [35]. We measured the interlayer interaction energy directly by varying the concentration of the binary mixtures by using a method that has been developed in our laboratory for its measurement [45]. The experimental results show that the energy difference Δ between the SmC^* and SmC_A^* phases and the slope of Δ with temperature decreases by increasing the ratio of the ferroelectric material MC452 in the mixtures, but the energy barrier between the two phases remains large. The results are rather different from the assumption made by Gorecka *et al.* of neglecting the quadrupolar term; that is, the quadrupolar term was assumed to be zero and the frustration state was due to an easy transformation from SmC_A^* to SmC^* and vice versa. The experimental results allow us to understand the mechanism of the gradual phase transition observed in the thin cell of the binary mixture where the apparent tilt angle is shown to change continuously with the field. The phase transition occurs through solitary-wave propagation, which can easily be prohibited by the friction of the surface effects. When Δ is small, solitary-wave propagation is easily suppressed and some parts of the cell remain in the metastable phase even after the temperature crosses the phase transition temperature. By increasing the temperature further, the phase transition occurs gradually via the boundary propagation. Hence the two phases coexist over a wide range of temperatures. Since the gradual phase transition is similar to the phenomenon of thresholdless antiferroelectric switching in the sense that one state transits to the other state gradually, thresholdless switching is naturally expected to arise from the same mechanism as the gradual phase transition. Actually, we observed thresholdless switching for the mixture near the critical concentration using a thick cell. The mechanism is the suppression of the solitary-wave propagation, the same as for the gradual phase transition. This is different from conventional models: continuous evolution of ϕ and the Langevin-like alignment of ϕ both with the field. We remark that the switching speed of thresholdless switching in the mixture close to the critical concentration is too slow to use in applications. We also provide better evidence for supporting the polarization stiffening model for observing ferroelectric V-shaped switching in a ferroelectric material MC452.

ACKNOWLEDGMENTS

We extend our grateful thanks to Mitsubishi Gas Chemicals Company, Inc. and Nissan Chemical Industries, Ltd. for donating their valuable liquid-crystal compounds and aligning agent, respectively. We thank Yu. P. Panarin for discussions, M. J. Sufin and U. Manna for assisting us in the experimental work. Results of V-shaped switching (Fig. 15) are taken from the works of A. D. L. Chandani, whom we acknowledge. We thank the Science Foundation of Ireland (SFI), Grant No. (02/IN.1/I.031), for funding the research work in Dublin. J.K.S. thanks Samsung Electronics Co., Ltd. for granting a leave of absence from Seoul.

[1] A. D. L. Chandani, E. Gorecka, Y. Ouchi, H. Takezoe, and A. Fukuda, Jpn. J. Appl. Phys., Part 2 **28**, L1265 (1989).
[2] A. Fukuda in *Proceedings, Asia Display* (SID, Tokyo, 1995), pp. 61–63.
[3] C. Tanaka, T. Fujiyama, T. Maruyama, and S. Nishiyama, in *Abstracts, 21st Japanese Liquid Crystal Conference*, (Japanese Liquid Crystal Soc., 1995), pp. 250–251.
[4] S. Inui, N. Iimura, T. Suzuki, H. Iwase, K. Miyachi, Y. Takanishi, and A. Fukuda, J. Mater. Chem. **6**, 671 (1996).
[5] T. Yoshida, T. Tanaka, J. Ogura, H. Wakai, and H. Aoki, SID Int. Symp. Digest Tech. Papers **28**, 841 (1997).
[6] R. Hasegawa, H. Fujiwara, H. Nagata, T. Saishu, R. Iida, Y. Hara, M. Akiyama, H. Okumura, and K. Takatoh, in *Proceedings, AM-LCD*, (SID, Tokyo, 1997), pp. 119–122.
[7] T. Verhulst, Jpn. J. Appl. Phys., Part 1 **36**, 720 (1997).
[8] M. Lu, K. H. Yang, and J. L. Sanford, Ferroelectrics **246**, 163 (2000).
[9] L. K. M. Chan, P. Bartelous, P. W. H. Surguy, N. Flannigan, G. Swedenkras, C. Waldelof, M. Rampin, A. Vindigni, I. Underwood, D. G. Vass, M. I. Newsman, J. M. Oton, and X. Quintana, in *Proceedings of the International Display Research Conference, 2000*, edited by P. J. Bos (Society of Infomation Display, Cambell, CA, 2000), pp. 261–264.
[10] S.-D. Lee and J.-H. Lee, in *Proceedings of the 4th International Display Research Conference, Nagoya, Japan, 1997*, edited by H. Uchiike (SID, Tokyo, 1997), pp. 69–72.
[11] H. Pauwels, B. Verweire, K. D'have, and J. Fornier, SID Int. Symp. Digest Tech. Papers **29**, 1175 (1998).
[12] T. Qian and P. L. Taylor, Phys. Rev. E **60**, 2978 (1999).
[13] L. A. Parry-Jones and S. J. Elston, Appl. Phys. Lett. **79**, 2097 (2001).
[14] N. J. Mottram and S. J. Elston, Phys. Rev. E **62**, 6787 (2000).
[15] N. J. Mottram and S. J. Elston, Liq. Cryst. **26**, 1853 (1999).
[16] A. de Vries, A. Ekachai, and N. Spielberg, Mol. Cryst. Liq. Cryst. **49**, 143 (1979).
[17] N. A. Clark, T. Bellini, R.-F. Shao, D. Coleman, S. Bardon, and D. R. Link, Appl. Phys. Lett. **80**, 4097 (2002).
[18] Y. Hattori, T. Fujiyama, T. Maruyama, C. Tanaka, H. Hama, and S. Nishiyama, in *Proceedings, AM-LCD* (SID, Tokyo, 1998), pp. 121–124.
[19] T. Matsumoto, A. Fukuda, M. Johno, Y. Motoyama, T. Yui, S.-S. Seomun, and M. Yamashita, J. Mater. Chem. **9**, 2051 (1999).
[20] M. Takeuchi, K. Chao, T. Ando, T. Matsumoto, A. Fukuda, and M. Yamashita, Ferroelectrics **246**, 1 (2000).
[21] Y. Yoshioka, M. Johno, T. Yui, and T. Matsumoto, European Patent Applied, EP1039329 (2000).
[22] J.-K. Song, A. D. L. Chandani, A. Fukuda, J. K. Vij, I. Kobayashi, and A. V. Emelyanenko, Phys. Rev. E **76**, 011709 (2007).
[23] M. Nakagawa and T. Akahane, J. Phys. Soc. Jpn. **55**, 1516 (1986).
[24] K. Okano, Jpn. J. Appl. Phys., Part 2 **25**, L846 (1986).
[25] A. D. L. Chandani, T. Hagiwara, Y. Suzuki, Y. Ouchi, H. Takezoe, and A. Fukuda, Jpn. J. Appl. Phys., Part 2 **27**, L276 (1988).
[26] N. A. Clark, D. Coleman, and J. E. Maclennan, Liq. Cryst. **27**, 985 (2000).
[27] M. Copic, J. E. Maclennan, and N. A. Clark, Phys. Rev. E **65**, 021708 (2002).
[28] P. Rudquist, J. P. F. Lagerwall, M. Buivydas, F. Gouda, S. T. Lagerwall, N. A. Clark, J. E. Maclennan, R. Shao, D. A. Coleman, S. Bardon, T. Bellini, D. R. Link, G. Natale, M. A. Glaser, D. M. Walba, M. D. Wand, and X.-H. Chan, J. Mater. Chem. **9**, 1257 (1999).
[29] P. Rudquist, J. P. F. Lagerwall, M. Buivydas, F. Gouda, S. T. Lagerwall, D. M. Walba, and N. A. Clark, SID Int. Symp. Digest Tech. Papers **30**, 409 (1999).
[30] B. Park, S.-S. Seomun, M. Nakata, M. Takahashi, Y. Takanishi, K. Ishikawa, and H. Takezoe, Jpn. J. Appl. Phys., Part 1 **38**, 1474 (1999).
[31] B. Park, M. Nakata, S.-S. Seomun, Y. Takanishi, K. Ishikawa, and H. Takezoe, Phys. Rev. E **59**, R3815 (1999).
[32] V. Manjuladevi, Yu. P. Panarin, and J. K. Vij, Appl. Phys. Lett. **91**, 052911 (2007).
[33] V. Manjuladevi, J. K. Vij, and Yu. P. Panarin, Mol. Cryst. Liq. Cryst. Suppl. Ser. **477**, 717 (2007).
[34] S.-S. Seomun, T. Gouda, Y. Takanishi, K. Ishikawa, H. Takezoe, and A. Fukuda, Liq. Cryst. **26**, 151 (1999).
[35] E. Gorecka, D. Pociecha, M. Glogarova, and J. Mieczkowski, Phys. Rev. Lett. **81**, 2946 (1998).
[36] D. Pociecha, M. Glogarova, E. Gorecka, and J. Mieczkowski, Phys. Rev. E **61**, 6674 (2000).
[37] K. Hiraoka, A. Taguchi, Y. Ouchi, H. Takezoe, and A. Fukuda, Jpn. J. Appl. Phys., Part 2 **29**, L103 (1990).
[38] N. M. Shtykov, A. D. L. Chandani, A. V. Emelyanenko, A. Fukuda, and J. K. Vij, Phys. Rev. E **71**, 021711 (2005).
[39] A. D. L. Chandani, N. M. Shtykov, V. P. Panov, A. V. Emelyanenko, A. Fukuda, and J. K. Vij, Phys. Rev. E **72**, 041705 (2005).
[40] N. Hayashi, T. Kato, T. Aoki, T. Ando, A. Fukuda, and S. S. Seomun, Phys. Rev. E **65**, 041714 (2002).
[41] N. Hayashi, T. Kato, T. Ando, A. Fukuda, S. Kawada, and S. Kondoh, Phys. Rev. E **68**, 011702 (2003).
[42] J.-K. Song, A. Fukuda, and J. K. Vij, Phys. Rev. Lett. **101**, 097801 (2008).

[43] M. A. Osipov and A. Fukuda, Phys. Rev. E **62**, 3724 (2000).
[44] A. V. Emelyanenko, A. Fukuda, and J. K. Vij, Phys. Rev. E **74**, 011705 (2006).
[45] J.-K. Song, A. Fukuda, and J. K. Vij, Phys. Rev. E **76**, 011708 (2007).
[46] L. A. Parry-Jones, E. Kriezis, and S. Elston, Mol. Cryst. Liq. Cryst. Suppl. Ser. **410**, 129 (2004).
[47] A. Fukuda, Y. Takanishi, T. Isozaki, K. Ishikawa, and H. Takezoe, J. Mater. Chem. **4**, 997 (1994).
[48] D. Pociecha, E. Gorecka, M. Cepic, N. Vaupotic, B. Zeks, D. Kardas, and J. Mieczkowski, Phys. Rev. Lett. **86**, 3048 (2001).
[49] N. Hiji, Y. Ouchi, H. Takezoe, and A. Fukuda, Jpn. J. Appl. Phys., Part 1 **27**, 8 (1988).
[50] S. S. Seomun, Y. Takanishi, K. Skarp, H. Takezoe, and A. Fukuda, Jpn. J. Appl. Phys., Part 1 **36**, 3586 (1996).
[51] K. Hiraoka, Y. Takanishi, K. Skarp, H. Takezoe, and A. Fukuda, Jpn. J. Appl. Phys., Part 2 **30**, L1819 (1991).
[52] N. M. Shtykov, J. K. Vij, R. A. Lewis, M. Hird, and J. W. Goodby, Phys. Rev. E **62**, 2279 (2000).
[53] S. Jaradat, P. D. Brimicombe, C. Southern, S. D. Siemianowski, E. DiMasi, M. Osipov, R. Pindak, and H. F. Gleeson, Phys. Rev. E **77**, 010701(R) (2008).
[54] T. Ando, Master thesis, Shinshu University, Japan, 2002.